COMPARATIVE STUDY OF 4(8)-PATH AND 5(10)-PATH CONFIGURATIONS FOR ATT FLOW MEASUREMENTS IN CIRCULAR CONDUITS

Sergey Marushchenko
sergii.maruschenko@hslu.ch
Lucerne University of Applied Sciences and Arts
Technikumstr. 21, CH-6048, Horw, Switzerland

Peter Gruber
peter.gruber@hslu.ch
Lucerne University of Applied Sciences and Arts
Technikumstr. 21, CH-6048, Horw, Switzerland
&
Rittmeyer Ltd , CH - 6340 Baar, Switzerland

INTRODUCTION

The IEC41 norm [1] on hydraulic efficiency is under a major revision. The Acoustic Transit Time (ATT) method for flow measurement, up to now classified only as a secondary method listed in the Annex, will move forward and will become a primary method for determining the flow in turbines and pump-turbines. Major upgrades include the introduction of the OWICS method for flow integration and the extension of recommended values of the number of acoustic paths *N*. The OWICS method is expected to improve for fully developed velocity profiles the flow integration accuracy in comparison with the Gauss-Jacobi method by the use of a more realistic velocity profile. An increase of the number of acoustic paths *N* is also expected to improve the accuracy of flow integration. Comparisons of the OWICS and Gauss-Jacobi methods have already been conducted in [2, 3]. However, it was done only for N=4 and for the analytically defined flow velocity profiles. The integration error ε of the OWICS and the Gauss-Jacobi methods as a function of *N* have also been carried out in [1]. However, these calculations were made only for fully developed flow velocity profiles. Therefore, the main objective of this study is to compare the performance of the Gauss-Jacobi and the OWICS methods, and the benefit of an increase of *N* under more realistic disturbed flow conditions.

1. GENERAL THEORY AND PROBLEM STATEMENT

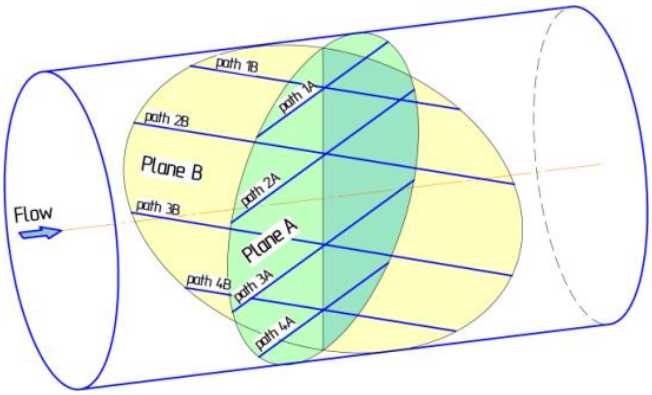

Fig. 1: Conventional ATT flow meter schematic

Figure 1 shows the schematic of a typical ATT flow meter installation. Conventionally, it consists of several acoustic paths which form two equal measuring planes. The most common number *N* of acoustic paths in one plane is 4, however, according to the latest IEC41 code revision, the recommended number of acoustic paths N is allowed to vary from 4 to 9. Two paths on the same level form a measuring layer, i.e. total number of measuring layers equals *N*. Double plane design is used to decrease the possible influence of cross flow on the accuracy of measurements.

In order to prevent possible misunderstandings, in the framework of the present paper, if nothing else is specified, the value *N* means the number of measuring paths in each measurement plane, i.e. the total number of measuring paths in a *N*-path flow meter is *2N*. Therefore also the abbreviation 4(8)-path in the title.

1.1 The area flow function

The total flow rate through a unit circle cross section can be approximated as a sum of the elementary flow rates passing through the number of horizontal layers (Fig. 1.2, left):

$$Q = \sum_{i=1}^{N} \Delta Q_i = \sum_{i=1}^{N} \bar{v}_{axi} \cdot l_i \cdot \Delta z \,, \tag{1}$$

where $\bar{v}_{axi}$: average axial velocity at i-th layer

l_i: projected path length (Fig. 1.2, right)

Δz: width of i-th layer

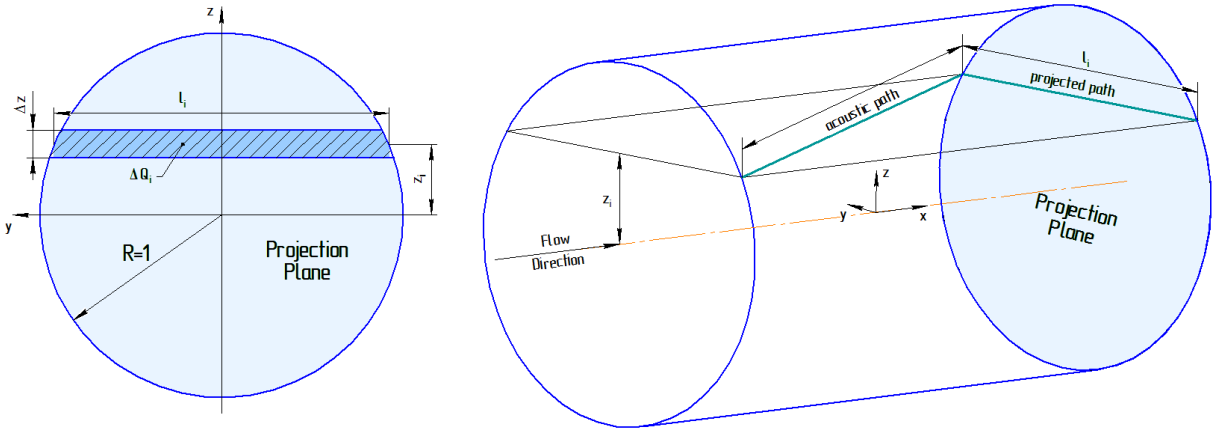

Fig. 2: Schematic of flow measurement in a regular pipe using the ATT technique with normalized radius of R=1

Tending the number of layers *N* to infinity, the sum in eq. (1) can be replaced by the integral:

$$Q = \lim_{N\to\infty} \sum_{i=1}^{N} \bar{v}_{axi} \cdot l_i \cdot \Delta z = \int_{-1}^{1} F(z) \cdot dz \,, \tag{2}$$

with $F(z) = \bar{v}_{ax}(z) \cdot l(z)$ (3)

The function $F(z)$ is called area flow function and describes the distribution of the partial flow rates through the elementary layers of the cross section and has dimension [m^2/sec]. A flowmeter has a finite number *N* of measuring layers, therefore, the integral in eq. (2) has to be replaced by a finite sum of *N* discrete values of $F(z_i)$. Conventionally, for that purpose the Gaussian quadrature method is used, because it has the highest polynomial degree of *2N-1* of all the existing quadrature methods The polynomial degree of a quadrature method indicates the highest order of a polynomial which can be integrated with zero error. Replacing the integral in eq. (1) by the *N*-point Gaussian quadrature leads to eq. (4) [2]:

$$Q \cong R \cdot \sum_{i=1}^{N} w_i \cdot \bar{v}_i \cdot l_i \,, \tag{1.4}$$

with w_i: weighting factor for i-th measuring layer

$\bar{v}_i$: averaged axial velocity at i-th measuring layer

l_i: projected path length

R: radius of circular section

1.2 Weighting and positioning

The highest polynomial degree of the Gaussian quadrature among existing quadratures obtained thanks to the specifically calculated positions of the quadrature nodes (corresponding to the heights z_i of the measuring layers). The positions z_i of the *N*-path Gaussian quadrature can be found as the zeros (roots) of the polynomial $p_N(z)$ generated by the recurrence relation:

$$p_N(z) = (z - a_{N-1}) \cdot p_{N-1}(z) - b_{N-1} \cdot p_{N-2}(z), \tag{5}$$

with $a_i = \dfrac{\int_{-1}^{1} F(z) \cdot z \cdot p_i^2(z) \cdot dz}{\int_{-1}^{1} F(z) \cdot p_i^2(z) \cdot dz}$, $b_i = \dfrac{\int_{-1}^{1} F(z) \cdot p_i^2(z) \cdot dz}{\int_{-1}^{1} F(z) \cdot p_{i-1}^2(z) \cdot dz}$.

The weighting factors w_i are calculated according to the equation:

$$w_i = \frac{1}{F(z_i)} \cdot \int_{-1}^{1} F(z) \cdot L_i(z) dz \tag{6}$$

where $L_i(z) = \prod_{\substack{j=1 \\ j \neq i}}^{N} \dfrac{z - z_j}{z_i - z_j}$.

As the positions and weights are defined during the stage of the meter installation, the future flow conditions and, particularly, the real area flow function F_{real} in the measurement section are, obviously, unknown. Therefore, in order to calculate the weights and positions an assumed are flow function F_{assum} is conventionally used in eqs. (5)-(6) for *F*. This assumed area flow function F_{assum} is determined based on the measurement section's geometry and an assumed velocity profile $v_{assum}(r)$. In the conventional Gauss-Jacobi method for circular section this profile is assumed uniform, which leads to a deviation of the integrated discharge from the true discharge in the case of fully developed flow. Therefore, Voser [2] proposed the OWICS method which uses the profile of eq. (7) for calculating the positions and weights. The N-path Gaussian quadrature method guaranties that polynomial deviations of order 2N-1 of the real area flow function F_{real} from the assumed area flow function F_{assum} can still be integrated with zero

$$v_{assum}(r) = \left(1 - \left(\frac{r}{R}\right)^2\right)^{0.1} \tag{7}$$

Table 1 shows the Gauss-Jacobi positions z_i / R for *N*=1..5 and corresponding weights w_i calculated according to the Gauss-Jacobi and OWICS methods. In practice, for OWICS method,

Due to practical reasons, usually the Gauss-Jacobi positions are used for the OWICS method and the weights are recalculated according the OWICS method taking into account the actual paths' positions. The sensitivity investigation of Tresch & al. [2] shows the negligible influence on the accuracy of such minor paths' shift.

	Gauss-Jacobi		OWICS	
N	z_i/R [-]	w_i [-]	z_i/R [-]	w_i [-]
1	0	1.570796	0	1,513365
2	0.5	0.906900	0,48795	0,890785
3	0 0.707107	0.785398 0.555360	0 0,695608	0,768693 0,553707
4	0.309017 0.809017	0.597566 0.369316	0,303783 0,799639	0,588228 0,371884
5	0 0.5 0.866025	0.523599 0.453450 0.261799	0 0,493266 0,858534	0,515768 0,448857 0,265433

Table 1: Path positions and weights for N=1,..5 [2]

1.3 Problem statement

The OWICS method will probably be approved for the flow integration by the latest revision of the IEC41 norm [1]. However, there is no data published which allows to conclude whether and under what circumstances the new OWICS method outperforms the conventional Gauss-Jacobi method in terms of accuracy. Hence, the first objective of this study is the comparison of the OWICS and Gauss-Jacobi methods in terms of integration accuracy.

One of the main features of numerical quadrature is that the integration accuracy grows with the number of quadrature nodes. This means that for the discharge integration the accuracy of the flow rate integration is expected to improve with the number of acoustic paths. The proposed revision of the IEC41 code extends the range of recommended number of acoustic paths (in previous version the N=4 meter was considered as basic). The first question is therefore: how much can be gained in terms of accuracy if N is increased from 4 to 5? It was mentioned above that in practice the OWICS method often uses the Gauss-Jacobi positions, which means, the only difference between the methods consists in the values of weights used. Unlike to this fact, an increase of the number of acoustic paths leads in many cases to the need of new sensors. Consequently, it is of high practical interest to the manufacturers to understand the benefits of changing the existing industry standards. Hence, the second objective of this study is to increase the number of measuring layers by one and compare the former basic 4-path arrangement with a 5-path. Here higher number of paths are not investigated here although installations of 9-path arrangements exist.

Drilled in acoustic transducers for ATT flow meters in circular section are usually designed for exact path positions z/R. At the moment transducers for $N \leq 4$ (and N=9) at Gauss-Jacobi positions are common. However, for a 5-path Gauss-Jacobi arrangement (Table 1) the transducer for the position of $z/R = 0.866025$ needs to be developed (the transducers for z/R=0; 0.5 are already used in 1- and 2-path arrangements correspondingly). If therefore the outer path of a 5-path arrangement could be shifted from the $z/R = 0.866025$ to the $z/R = 0.809017$ position (Fig. 3) which corresponds to the outer path of a 4-path arrangement (Table 1), the necessity to develop a new transducer could be avoided. This not negligible shift affects the accuracy of the flow rate integration as the Gaussian quadrature requires specifically calculated quadrature nodes. The third objective of this study is therefore to evaluate the performance of a 5-path arrangement with shifted outer paths, in the framework of this paper referred to as 5(4)-path arrangement.

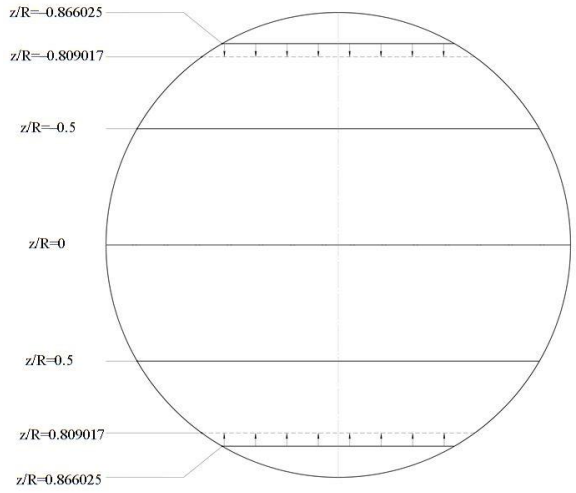

Fig. 3: Gauss-Jacobi 5-path (solid lines) outer path shift to 4-path position (dashed line)

2. THE ACCURACY OF FLOW INTEGRATION INVESTIGATION

2.1 Research methodology

Considering the objectives stated in the previous section, the following arrangements were selected for a comparative study:

- Gauss-Jacobi 4-path
- Gauss-Jacobi 5-path
- Gauss-Jacobi 5(4)-path
- OWICS 4-path
- OWICS 5-path

In the OWICS configurations the acoustic paths are arranged according to the Gauss-Jacobi method and the weights are recalculated according to the OWICS method for the Gauss-Jacobi positions. The summary of the path positions z_i / R and the weights w_i for selected configurations are presented in Table 2.

	Gauss-Jacobi 4-path		Gauss-Jacobi 5-path		Gauss-Jacobi 4(5)-path		OWICS 4-path		OWICS 5-path	
	z_i/R[-]	w_i[-]	z_i/R[-]	w_i[-]	z_i/R[-]	w_i[-]	z_i/R[-]	w_i[-]	z_i/R[-]	w_i[-]
Path 1	-0,809017	0,369317	-0,866025	0,261799	-0,809017	0,315435	-0,809017	0,365222	-0,866025	0,265433
Path 2	-0,309017	0,597566	-0,5	0,453449	-0,5	0,346402	-0,309017	0,598639	-0,5	0,448857
Path 3	0,309017	0,597566	0	0,523598	0	0,599994	0,309017	0,598639	0	0,515768
Path 4	0,809017	0,369317	0,5	0,453449	0,5	0,346402	0,809017	0,365222	0,5	0,448857
Path 5			0,866025	0,261799	-0,809017	0,315435			0,866025	0,265433

Table 2: The summary of the path positions z_i / R and the weights w_i for selected configurations

The following integration error ε (eq. 8) is used as performance criterion:

$$\varepsilon = \frac{Q - Q_{ref}}{Q_{ref}} \cdot 100\% \tag{8}$$

For the investigation of the integration error, the measured velocity values $\bar{v}_i$ and the reference flow rate value Q_{ref} are needed as input data. This data is obtained from numerical simulation. The study of the selected configuration's performances is divided into two logical parts. In the first part the performance of the selected configurations is studied for the example of the flow downstream of elbow-type disturbers: straight pipe (for reference), single 90° elbow, double 90° elbow in plane and double 90° elbow out of plane (Fig. 4). For each disturber two installation positions are studied: 2D and 5D downstream the disturber And three different Reynolds numbers are considered: 10^5, 10^6 and 10^7. Additionally, at each installation position the azimuthal installation angle α of the meter is varied from 0 to 180° in 15° steps in order to investigate the installation angle effect.

In the second part of study the performance of the selected configurations is studied for the example of the simulated flow in the Aratiatia hydraulic power plant water intake Hug & al. [4] (Fig. 5). This part investigates the meter performance for different hydraulic conditions in a real plant.

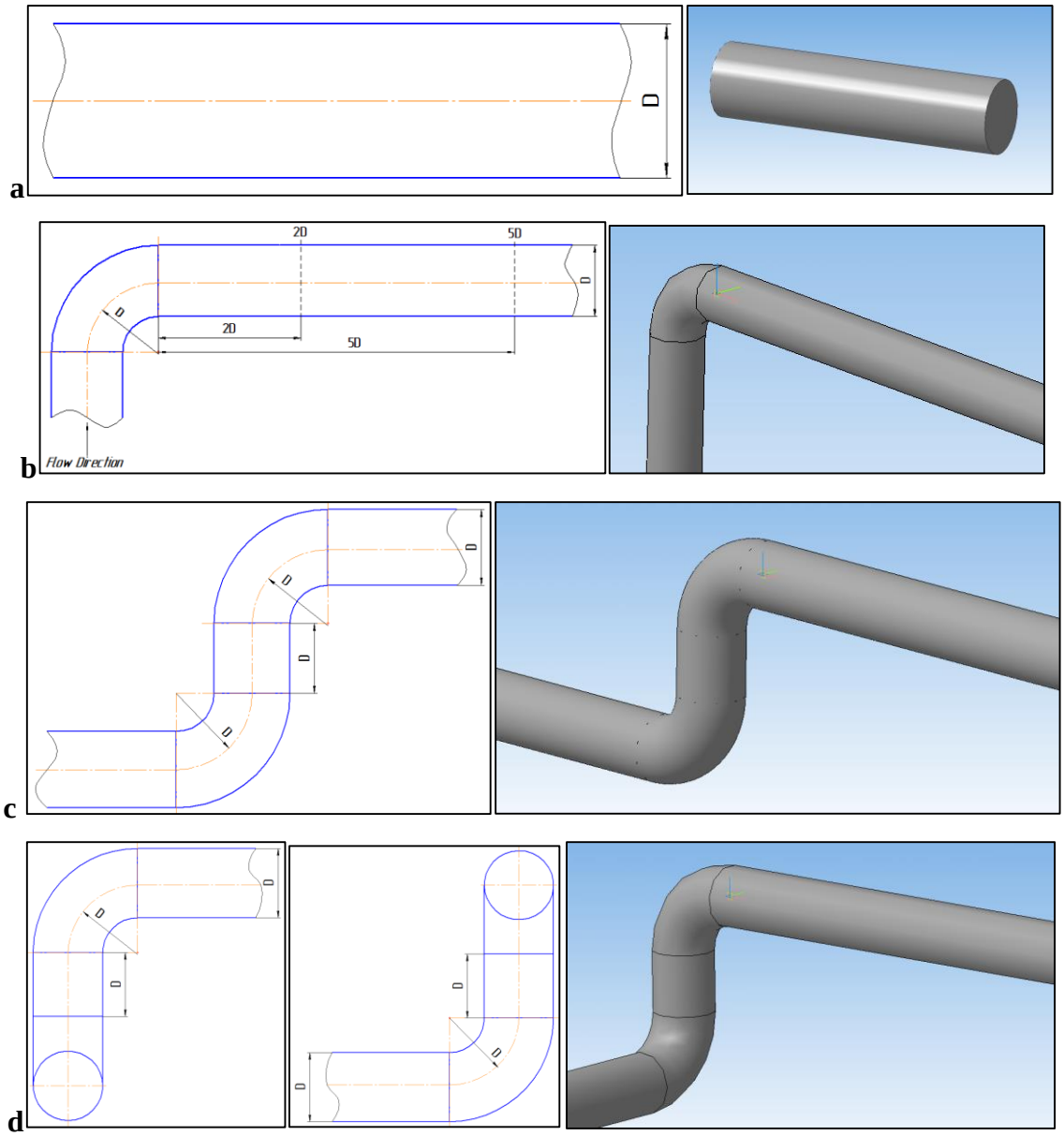

Fig. 4: Investigated disturbers` schematics and 3D models: a: straight pipe; b: single 90° elbow; c: double 90° elbow in plane; d: double 90° elbow out of plane

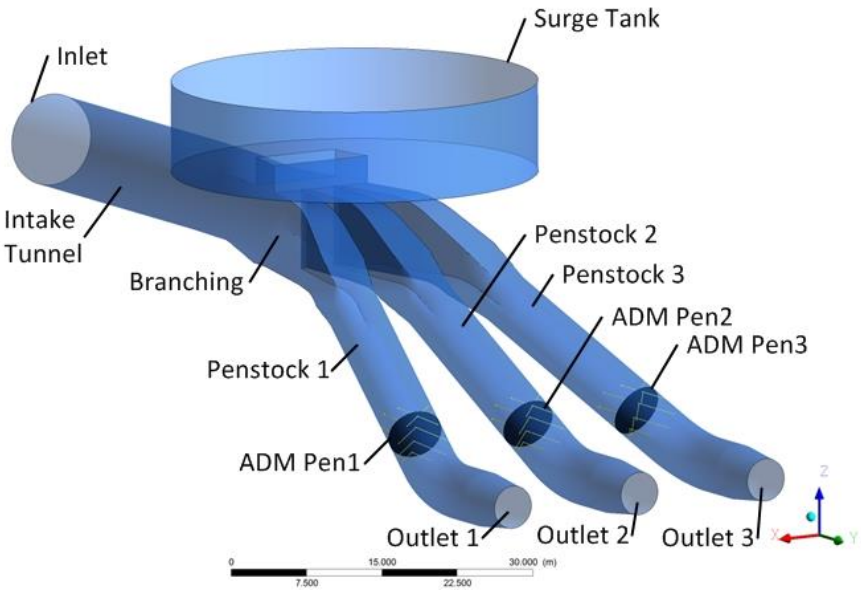

Fig. 5: Aratiatia hydraulic power plant schematic

2.2 Performance investigation on example of elbow-type disturbers

2.2.1 Numerical simulation of flow downstream the selected disturbers

The main data of the simulated flow are:
Pipe diameter: D = 0.5 m
Reynolds number Re: 10^5, 10^6, 10^7
Flow velocity: 0.2, 2, 20 m/s

The numerical simulation was performed with the ANSYS Fluent 14.5.7 software. The computational O-grid mesh with $2x10^6$ cells was developed in ANSYS ICEM CFD 14.5.7. The flow was simulated implementing the SST (Shear Stress Transport) model. For the inlet boundary condition of the computational domain the fully developed velocity profile shown in Fig. 2.3 is used. This profile was obtained from numerical simulation of the flow in a straight pipe of 5D length with translational periodic boundary conditions.

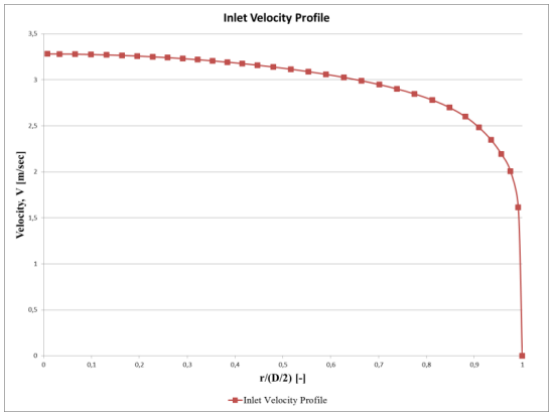

Fig. 6: Fully developed velocity profile used for inlet boundary condition definition

2.2.2 Results and discussion

Figure 7 shows the simulated velocity contours in a periodic straight pipe. The integration error values for a straight pipe are presented in Table 2.2.

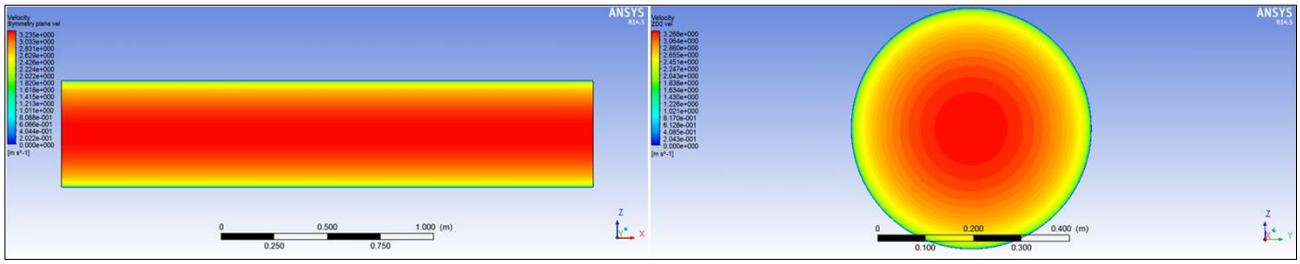

Fig. 7: Simulated mean velocity contours in straight pipe

	4-path		5-path		5(4)-path
	G-J	OWICS	G-J	OWICS	G-J
ε [%]	0,27	0,14	0,20	0,13	0,23

Table 3: Integration error values for fully developed flow in the straight pipe

Figures 8-10 show the simulation results for the selected disturber together with the integration error values of each studied arrangement as a function of the installation angle α and a Reynolds number of 10^5. In the appendix the simulation results are shown for the Gauss-Jacobi methods and Re=10^6 and $10^{7.}$ Additionally, each graph contains marked with colored circles "eps_average"-values, the error value averaged over all the installation angle. In order to simplify the perception of the data presented in Fig. 8-10 and Table 3, the summary of the average integration error $\bar{\varepsilon}$ and the error dispersion ε_{disp} (difference between minimal and maximal error values over all angles), for each disturber and configuration are shown in Table 4.

From the summary presented in Table 2.3, Fig. 8-10 and the appendix, the following observations can be made:

1. The OWICS method has a smaller average error value $\bar{\varepsilon}$ than the Gauss-Jacobi method. The error dispersion value ε_{disp}, however, is virtually independent on the method used.
2. A increase of the number of acoustic paths *N* from 4 to 5 significantly (up to 50%) decreases the average integration error $\bar{\varepsilon}$.
3. The meter installation at the 5D downstream position does not improve the average error value $\bar{\varepsilon}$, however, the error dispersion ε_{disp} significantly (up to 60%) decreases in comparison with 2D downstream the elbow.
4. For each disturber and position (2D, 5D) a specific range of angle of installation can be defined which minimizes the integration error under the assumption that the simulation is correct.
5. The variation of the Reynolds number does not show a clear trend.

The Gauss-Jacobi 5(4)-path arrangement usually performs worse than the Gauss-Jacobi 4-path arrangement in terms of average integration error $\bar{\varepsilon}$. The error dispersion value of this arrangement is not definitely better or worse than the Gauss-Jacobi 4-path arrangement's, however is significantly worse than Gauss-Jacobi 5-path arrangement's.

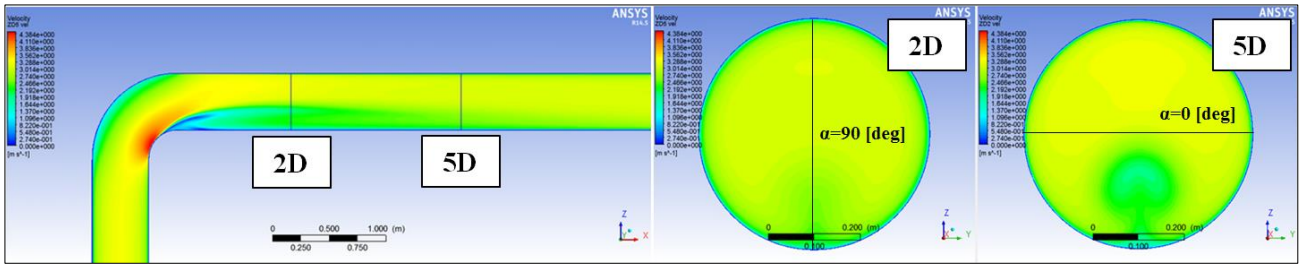

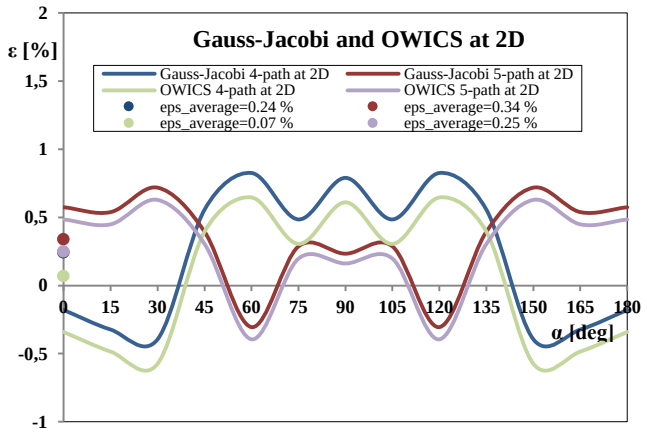

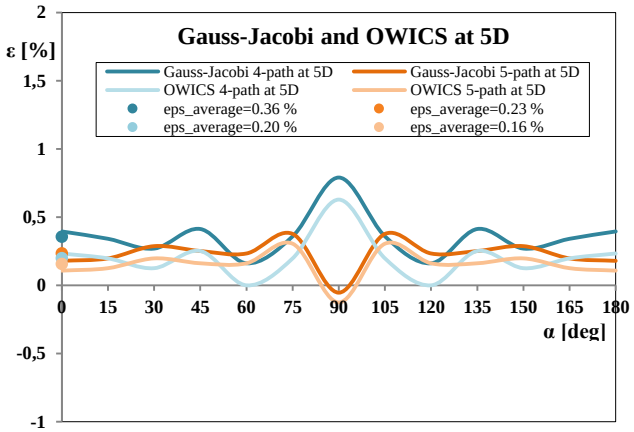

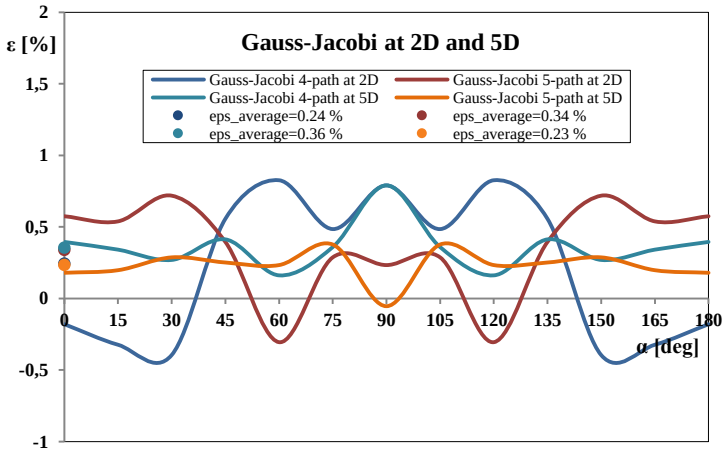

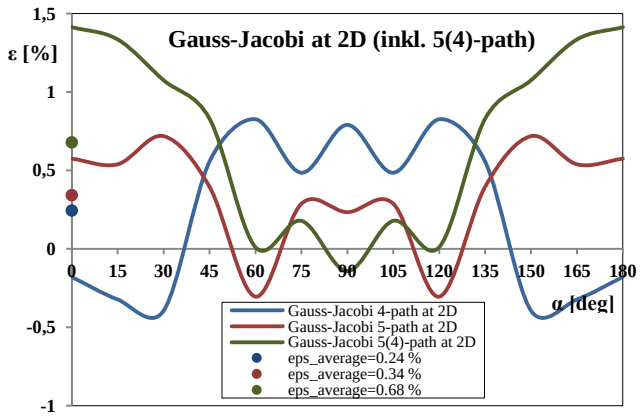

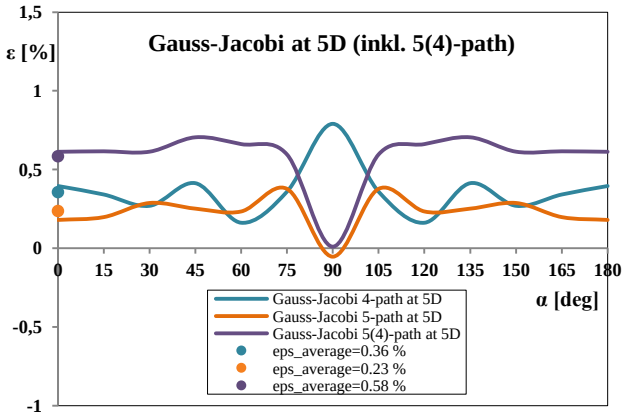

Fig. 8: Integration error values for single elbow, $Re=10^5$

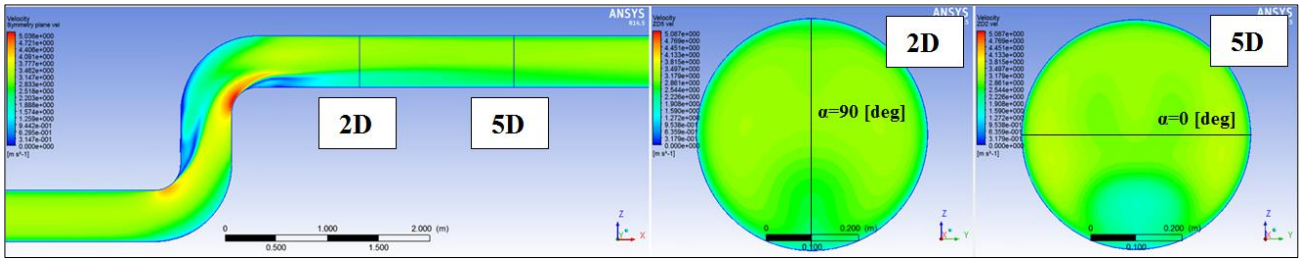

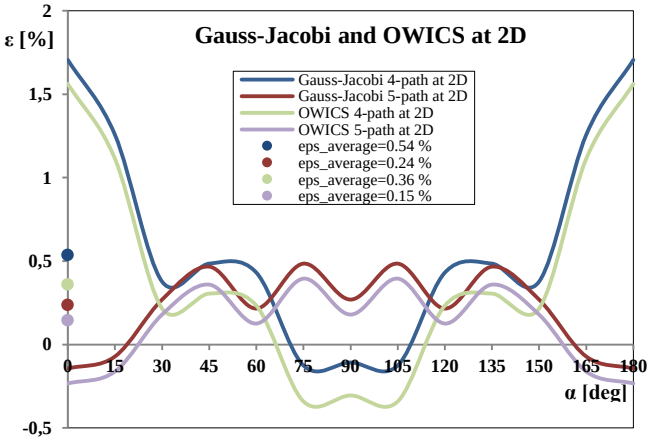

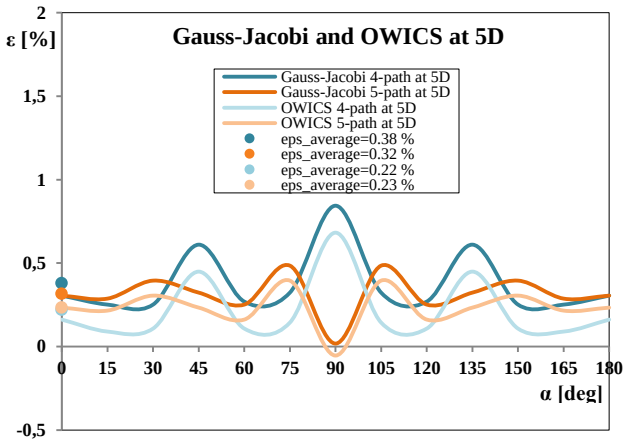

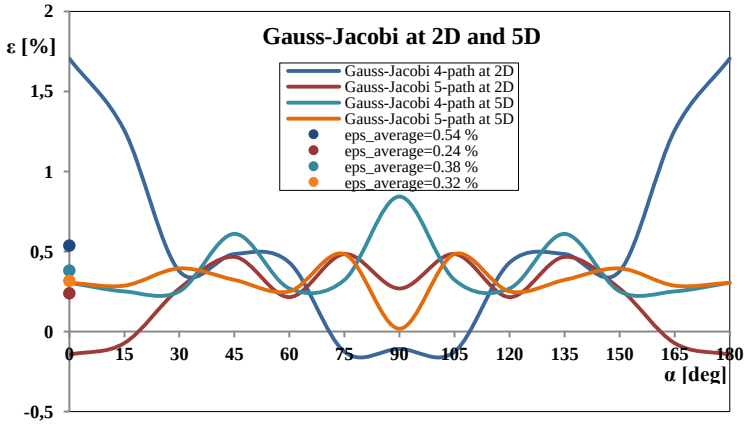

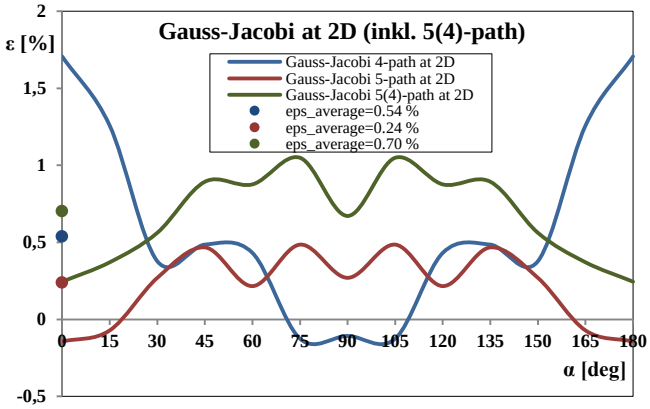

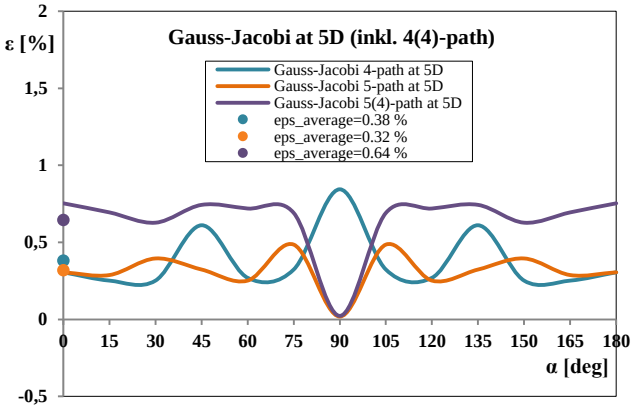

Fig. 9: Integration error values for double elbow in plane, Re=10^5

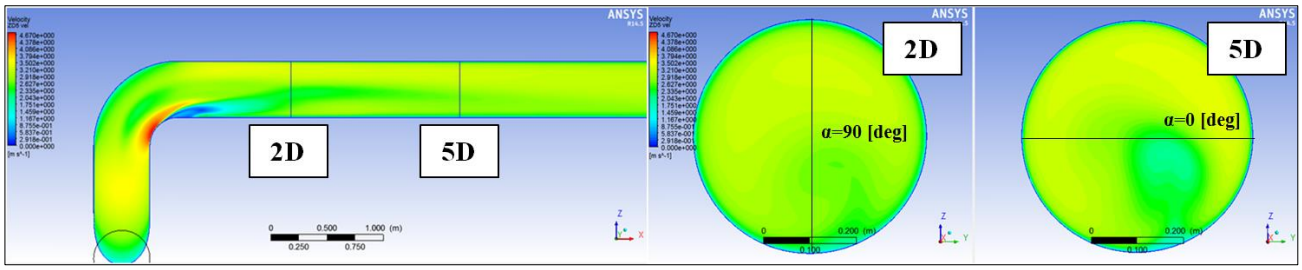

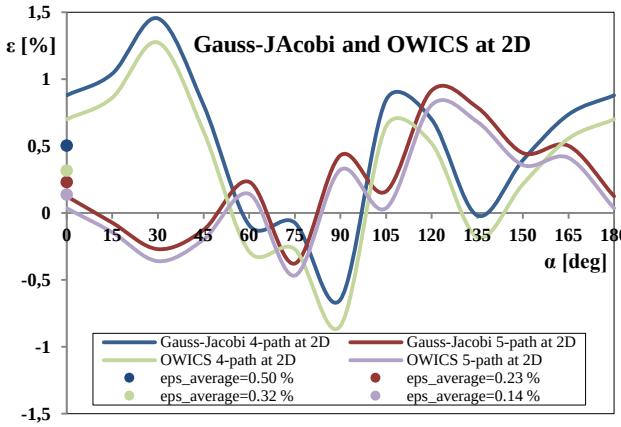

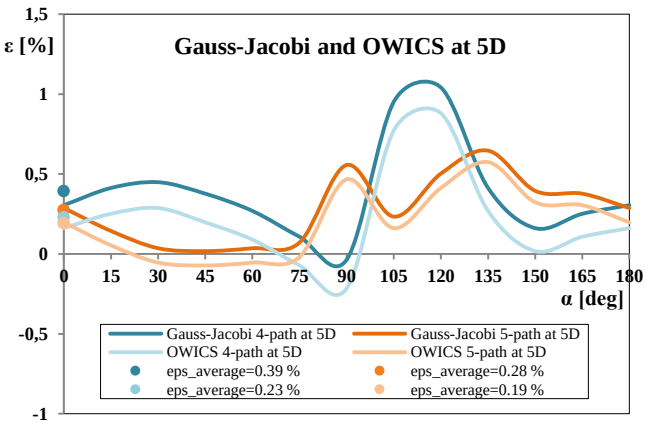

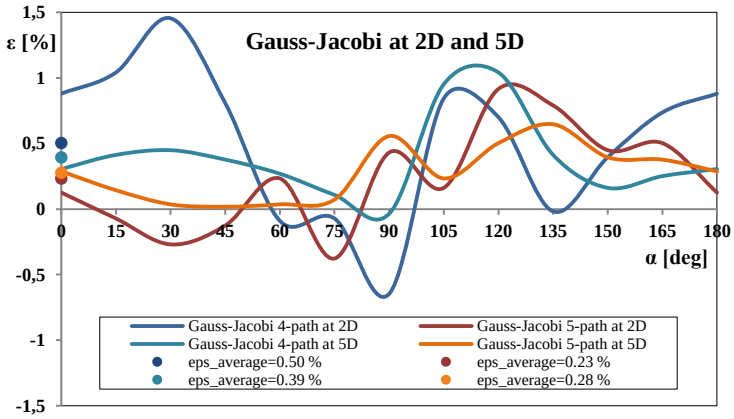

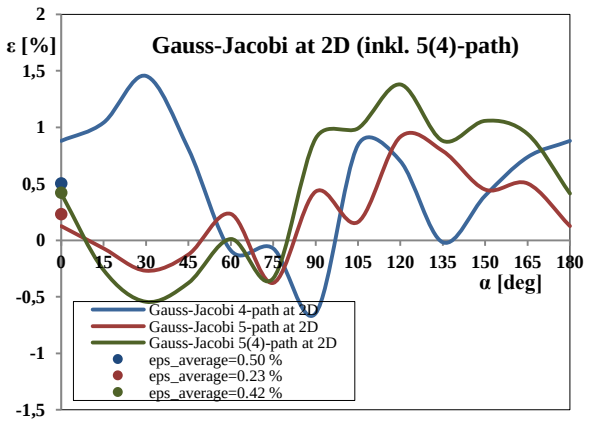

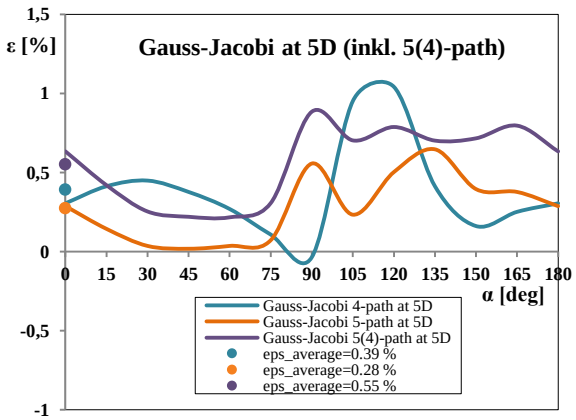

Fig. 10: Integration error values for double elbow out of plane, Re=10^5

			4-path				5-path				5(4)-path	
			Gauss-Jacobi		OWICS		Gauss-Jacobi		OWICS		Gauss-Jacobi	
			2D	5D	2D	5D	2D	5D	2D	5D	2D	5D
Straight pipe	Re=10^5	$\bar{\varepsilon}$ [%]	0,27		0,14		0,20		0,13		0,23	
		ε_{disp} [%]	-		-		-		-		-	
Single Elbow	Re=10^5	$\bar{\varepsilon}$ [%]	0,24	0,36	0,07	0,20	0,34	0,23	0,25	0,16	0,68	0,58
		ε_{disp} [%]	1,22	0,63	1,22	0,63	1,02	0,43	1,02	0,43	1,56	0,69
	Re=10^6	$\bar{\varepsilon}$ [%]	0.87	0.48	0.70	0.32	0.21	0.27	0.12	0.18	-	-
		ε_{disp} [%]	2.46	0.92	2.45	0.92	1.05	0.32	1.05	0.31	-	-
	Re=10^7	$\bar{\varepsilon}$ [%]	0.45	0.41	0.28	0.25	-0.15	0.19	-0.25	0.11	-	-
		ε_{disp} [%]	2.50	0.88	2.49	0.89	2.32	1.15	2.32	1.14	-	-
Double elbow in plane	Re=10^5	$\bar{\varepsilon}$ [%]	0,54	0,38	0,36	0,22	0,24	0,32	0,15	0,23	0,70	0,64
		ε_{disp} [%]	1,83	0,59	1,90	0,59	0,63	0,47	0,63	0,45	0,80	0,73
	Re=10^6	$\bar{\varepsilon}$ [%]	0.1	0.82	-0.09	0.66	0.06	0.09	-0.02	0.01	-	-
		ε_{disp} [%]	2.41	0.78	2.41	0.77	2.46	0.73	2.45	0.72	-	-
	Re=10^7	$\bar{\varepsilon}$ [%]	0.86	0.40	0.67	0.24	0.54	0.31	0.45	0.22	-	-
		ε_{disp} [%]	1.89	0.49	1.89	0.49	0.49	0.32	0.49	0.32	-	-
Double elbow out of plane	Re=10^5	$\bar{\varepsilon}$ [%]	0,50	0,39	0,32	0,23	0,23	0,28	0,14	0,19	0,42	0,55
		ε_{disp} [%]	2,10	1,08	2,12	1,10	1,29	0,63	1,28	0,65	1,92	0,67
	Re=10^6	$\bar{\varepsilon}$ [%]	0.19	0.46	0.01	0.30	0.33	0.27	0.25	0.18	-	-
		ε_{disp} [%]	2.08	2.73	2.07	2.74	0.91	2.13	0.91	2.12	-	-
	Re=10^7	$\bar{\varepsilon}$ [%]	0.11	0.07	-0.08	-0.06	0.24	0.25	0.15	0.16	-	-
		ε_{disp} [%]	1.43	1.69	1.43	1.67	1.56	1.37	1.55	1.36	-	-

Table 4: Average integration error $\bar{\varepsilon}$ and error dispersion ε_{disp} values summary

2.3 Performance investigation for the Aratiatia power plant

2.3.1 Numerical flow simulation at Aratiatia power plant

The simulations were performed with ANSYS CFX 12.0.
Three different operating conditions were simulated:
– Test 1: 3x90 m3/s (all three turbines in operation)
– Test 2: 2x90 m3/s (turbine 1 and 2 in operation, turbine 3 shutdown)
– Test 3: 1x50 m3/s (turbine 1 in operation, turbine 2 and 3 shutdown)

The boundary conditions for these operating points are listed below:

Inlet: The straight intake tunnel of the power plant is about 50 diameters long with constant circular cross section. The range of the Reynolds numbers lies between $Re=7\cdot10^6$ and $4.3\cdot10^7$ for the investigated operating points. Consequently, a fully developed velocity profile can be assumed at

the inlet to the simulation domain. This profile is calculated beforehand for each of the given flow rates in a separate simulation with a 2 diameter short straight section with translational periodic boundary conditions. These velocity distributions as well as the turbulence quantities are then used as inlet conditions for the main simulations.

Outlets: The number of outlets varies from 1 to 3 outlets depending on the operating conditions. The mass flow is set for each of the outlets. The outlet mass flows then are linked to the mass flow at the inlet in order to satisfy the mass flow balance. The expressions in the brackets show the boundary conditions, which are set at the outlet.
Test 1: All three outlets have the same mass flow.
Test 2: Outlet 1 and 2 have the same mass flow. Outlet 3 is defined as a no slip wall. This is a simplification, in reality the domain ends in the spiral casing upstream of the closed guide vanes.
Test 3: Outlet 1 and inlet have the same mass flow. Outlet 2 and 3 are defined as no slip walls.
Wall. The wall is specified as a no slip wall assuming hydraulically smooth surfaces.

Free surface: The free surface of the surge tank is defined as a free slip wall. This means that the water level is constant and the water has no friction at this boundary.

2.3.2 Meter performance at Aratiatia power plant

In Table 5 the integration errors ε for different simulated cases are shown. The code for the cases is as follows: the first number (1, 2 or 3) indicates how many penstocks are in operating, the second number (50, 90 or 110) indicates the flow rate, the term in brackets (1+2 or 1+3) indicates which of 3 penstocks are in operating, the last part of the code (P1 or P2) tells which penstock is evaluated.

The best result in the string is marked with the green color, the worst with the red color.

	Integration error ε [%]				
	Gauss-Jacobi 4-path [%]	Gauss-Jacobi 5-path [%]	Gauss-Jacobi 5(4)-path [%]	OWICS 4-path [%]	OWICS 5-path [%]
1x50_P1	1,09	-0,46	0,46	0,91	-0,56
1x50_P2	0,16	0,34	-0,21	0,00	0,03
2x90(1+2)_P1	-0,99	0,86	-1,27	-1,17	0,75
2x90(1+2)_P2	0,30	0,02	-0,14	0,14	-0,08
2x90(1+3)_P1	0,27	0,18	-0,36	0,10	0,08
3x50_P1	1,02	-0,28	0,54	0,84	-0,37
3x50_P2	1,04	-0,03	-0,19	0,91	-0,12
3x90_P1	0,97	-0,35	0,60	0,80	-0,45
3x90_P2	0,91	0,08	-0,18	0,77	0,00
3x110_P1	0,96	-0,37	0,62	0,78	-0,47
3x110_P2	0,86	0,11	-0,17	0,72	0,03
$\overline{\varepsilon}$ [%]	0.60	0.01	-0.03	0.44	-0.10

Table 5: Integration error summary for Aratiatia installation

As can be seen from the Table 5, the worst configuration is the Gauss-Jacobi 4-path. The best performance exhibits the Gauss-Jacobi 5-path configuration. The OWICS 5-path configuration has the best result in 4 cases out of 11. So the OWICS method superiority over the Gauss-Jacobi is not confirmed. If the penstocks are operated in a symmetrical mode, OWICS outperforms the Gauss-Jacobi configuration indicating that OWICS is more suitable for less disturbed flow profiles. The

accuracy improvement by increasing N is confirmed, as well as that a 4(5)-path configuration is useless.

CONCLUSION

In the first part the performance of different measuring configurations was investigated with the example in the presence of different elbow-type disturbers upstream of the measurement section. The obtained results show a definite superiority of the OWICS integration method over the Gauss-Jacobi method in terms of the average error $\bar{\varepsilon}$. Additionally, the results confirm that the increase of the number of acoustic paths from 4 to 5 decreases the average integration error $\bar{\varepsilon}$ and the error dispersion ε_{disp}. Furthermore, the effect of the flow disturbance intensity on the error dispersion value is observed: at 5D installation location the integration error dispersion values ε_{disp} are significantly smaller than the corresponding values at 2D. However, a larger distance from the disturber does not improve the average error $\bar{\varepsilon}$. It's cause could be the result of a systematic inaccuracy in the weighting and positioning procedures, as even in case of the straight periodic pipe, where the flow is fully developed, the integration error is still present (Table 2.3). For each disturber and position (2D, 5D) a specific range of angle of installation can be defined which minimizes the integration error under the assumption that the simulation is correct. If no simulation is available or if it is too inaccurate, the average integration error $\bar{\varepsilon}$ together with its dispersion ε_{disp} is a good estimate of what kind of accuracy range can be expected. The first part of the study also demonstrates that the Gauss-Jacobi 5(4)-path arrangement is worthless, as in terms of the average error $\bar{\varepsilon}$ value it performs even worse than Gauss-Jacobi 4-path arrangement.

In the second part, the performance of a specific measuring configurations was studied on the simulated flow of the Aratiatia power plant in New Zealand. The results from the Table 5, unlike the ones of Table 4 don't show a definite superiority of the OWICS over the Gauss-Jacobi method. However, they also confirm that by increasing the number N of measuring paths from 4 to 5 the integration error value decreases. It is also demonstrated, that the 5(4)-path arrangement is inferior. In the cases with symmetrical operation of the power plant, the OWICS integration error for 5-paths for the middle pipe P2 is on the average superior to the other methods.

REFERENCES

[1] IEC 60041 International Standard / International Electrotechnical Commission, Geneva, Switzerland, 1991

[2] T. Tresch, P. Gruber, T. Staubli: Comparison of integration methods for multipath acoustic discharge measurements, IGHEM 2006, Portland, http://www.ighem.org/ Paper2006/d6. pdf

[3] A.Voser Analyse und Fehleroptimierung der mehrpfadigen akustischen Durchflussmessung in Wasserkraftanlagen, ETH Zürich Dissertation Nr. 13102, 1999

[4] S. Hug, T. Staubli, P. Gruber: Comparison of measured path velocities with numerical simulations for heavily disturbed velocity distributions, IGHEM 2012, Trondheim

Appendix: Velocity distributions after the disturber and integration errors for the Gauss-Jacobi methods for Reynolds number of 10^6 and 10^7 (10^5 is already in main body Fig. 8-10)

Single elbow

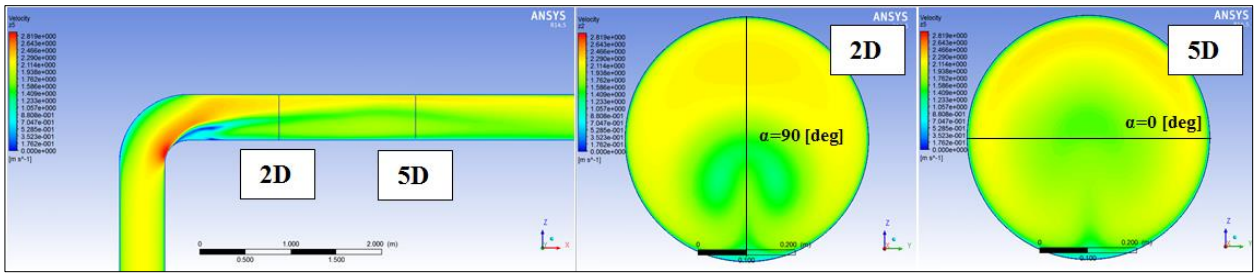

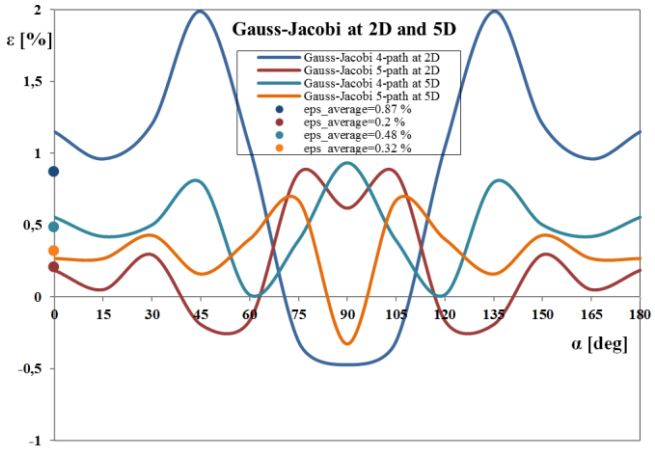

Re=10^6

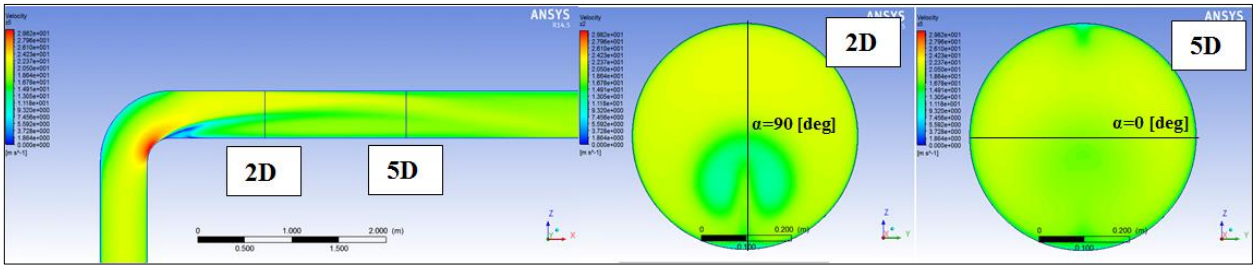

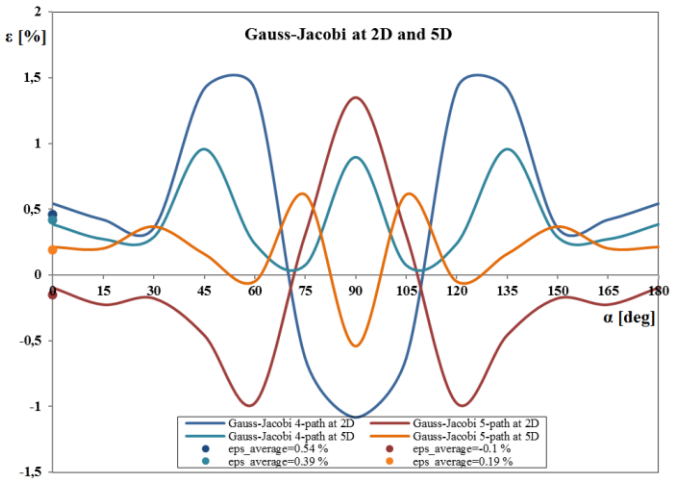

Re=10^7

Double elbow in plane

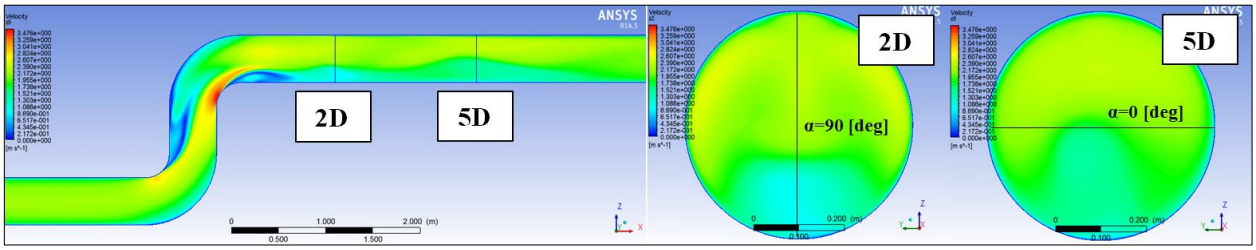

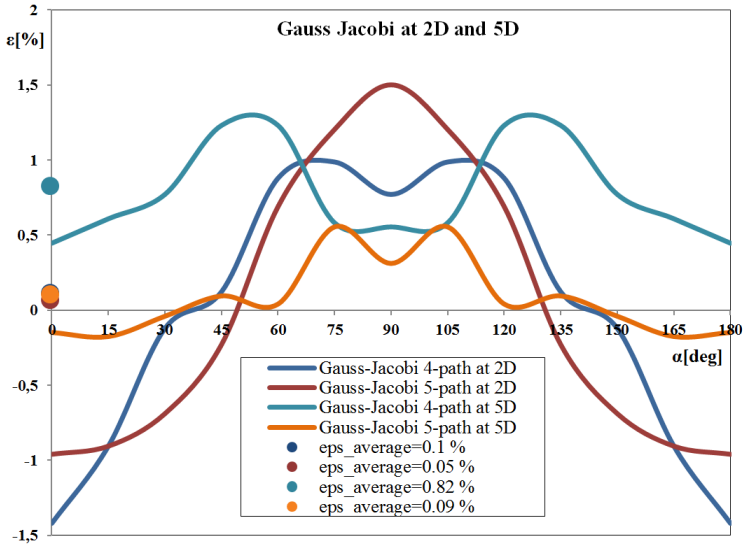

Re=10^6

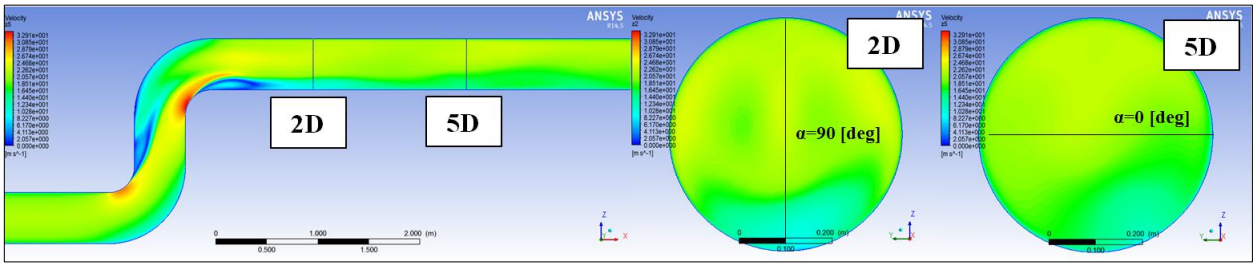

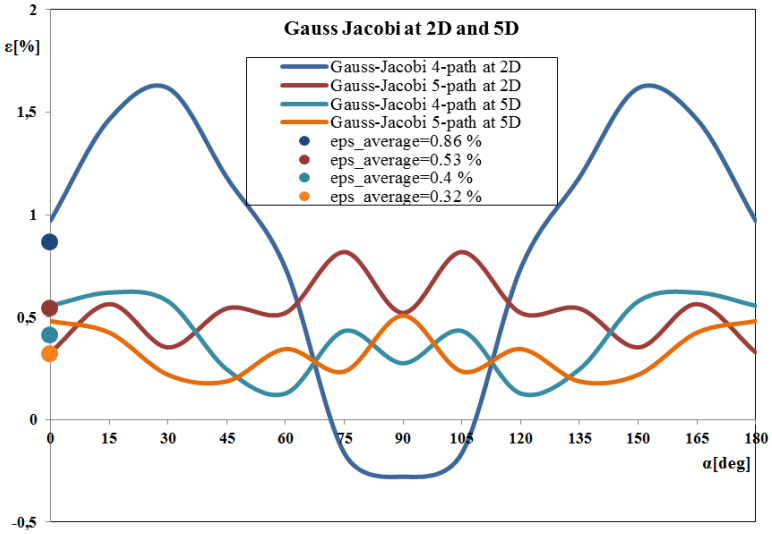

Re=10^7

Double elbow out of plane

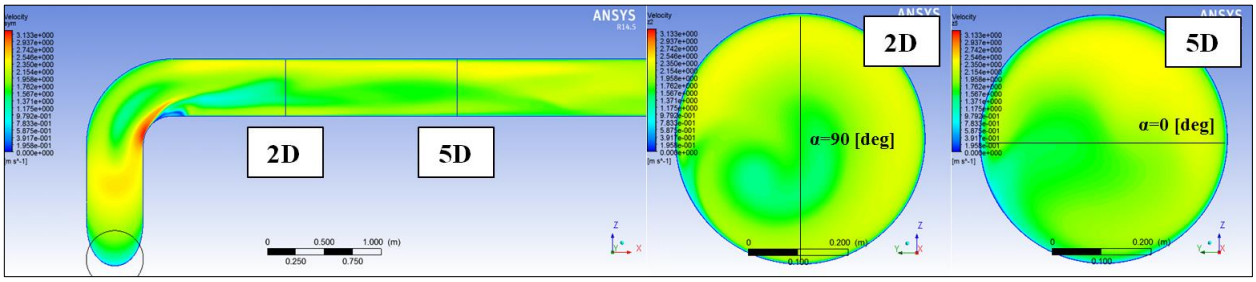

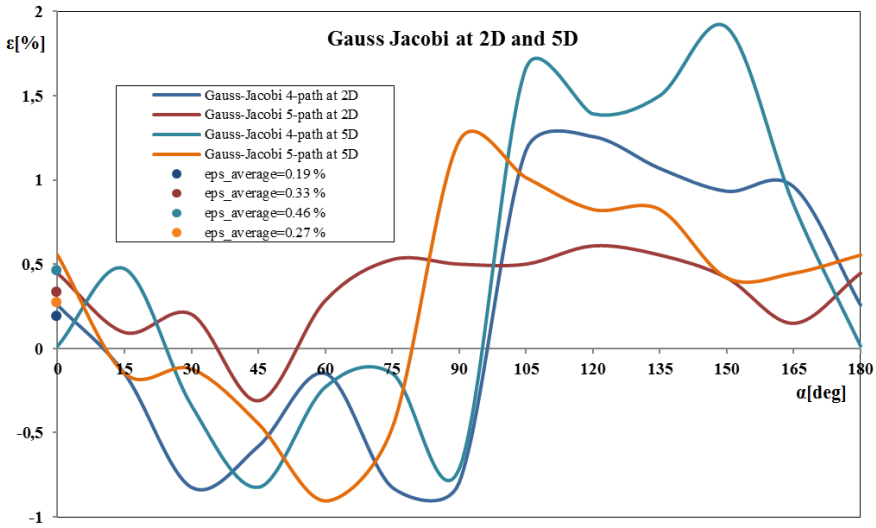

Re=10^6

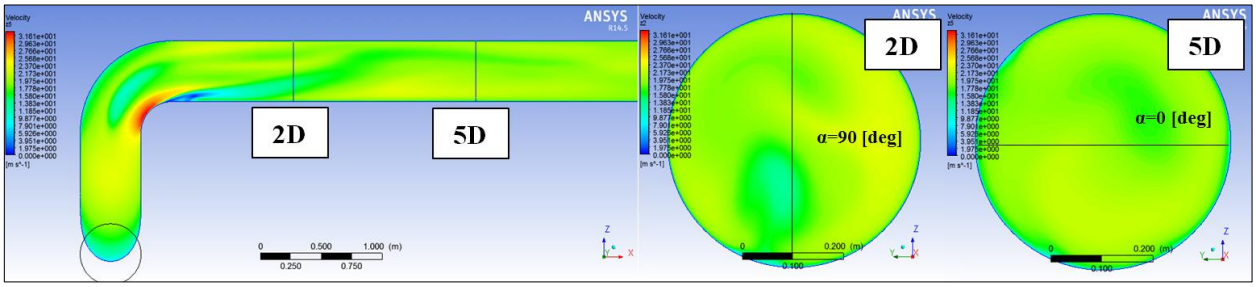

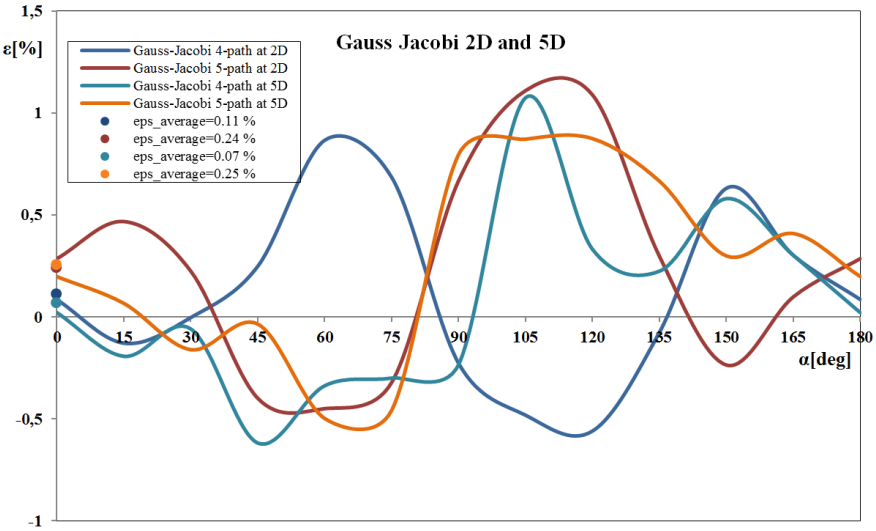

Re=10^7